Journal of Physics: Conference Series **92** (2007) 012011 doi:10.1088/1742-6596/92/1/012011

SASER action in optically excited ruby: Angular and spectral distribution

L G Tilstra, A F M Arts and H W de Wijn

Department of Physics and Astronomy, and Debye Institute, Utrecht University, PO Box 80.000, 3508 TA Utrecht, The Netherlands

E-mail: l.g.tilstra@sron.nl, h.w.dewijn@phys.uu.nl

Abstract. Selective pulsed optical excitation is used in 500-at.ppm ruby (Al_2O_3:Cr^{3+}) at 1.4 K to prepare complete population inversion of the Zeeman-split $\overline{E}(^2E)$ doublet in a zone of limited size. The inversion results in prolific stimulated emission of phonons resonant with the one-phonon transition connecting the doublet states. The phonons are detected via the R_1 luminescence. The angular and spectral distributions of the associated acoustic wave are measured using a geometry with inverted zones at either end of the crystal, one serving as generator and the other as detector. The divergence appears to be governed by the geometry of the zone, while the spectral distribution is, within errors, in keeping with the inhomogeneously broadened phonon transition.

In a single crystal of dilute ruby (Al_2O_3:Cr^{3+}) held below 2 K, phonon avalanches may be created by population inversion of the metastable $\overline{E}(^2E)$ doublet split by a magnetic field. As depicted in figure 1(a), the inversion can be accomplished by selective pulsed optical pumping out of the $^4A_2$ ground multiplet into the *upper* state of the $\overline{E}(^2E)$ doublet (denoted by E_+). The subsequent one-phonon decay to the *lower* $\overline{E}(^2E)$ state (E_-) releases a resonant phonon. In previous work [1], we have shown that the decay process is coherent, i.e., the associated acoustic wave is coupled to the *transverse* spin components, and leads to an avalanche of phonons by repeated stimulated emission, provided Cr^{3+} residing in E_+ are available in sufficient density. The phonons created may be measured via the R_1 luminescence emanating from E_-. In longer crystals, such that the zone of excited Cr^{3+} is narrow and of limited depth as a result of optical absorption, the generated phonons are observed to form a collimated beam that reverberates between the crystalline end faces, and engages in further amplification each time it passes through the inverted zone [2]. The ruby system thus acts as a saser.

In the present experiments, designed to study the angular divergence and the spectral width of the acoustic wave, we examine the wave after it has migrated to a second excited zone at the opposite end of the crystal, as shown in figure 1(b). The right zone serves as generator, the left zone as luminescent detector. This arrangement allows us to measure the angular divergence of the acoustic wave upon taking advantage of mutual lateral displacements, and its spectral distribution by the use of a magnetic gradient field separating the center frequencies.

The specimen is a cuboidal Czochralski-grown single crystal of ruby, $6.60\times4.63\times1.91$ mm^3 in size. The Cr^{3+} concentration is 500 at.ppm, or 1.2×10^{25} m^{-3}. The crystalline a axis is parallel to the longest edges, while the c axis makes an angle of 25° with the main faces and the middle dimension. The surface roughness is of order 10 nm, much smaller than the 135-nm phonon wavelength. The crystal, immersed in liquid He at 1.4 K to freeze out thermal relaxation, was

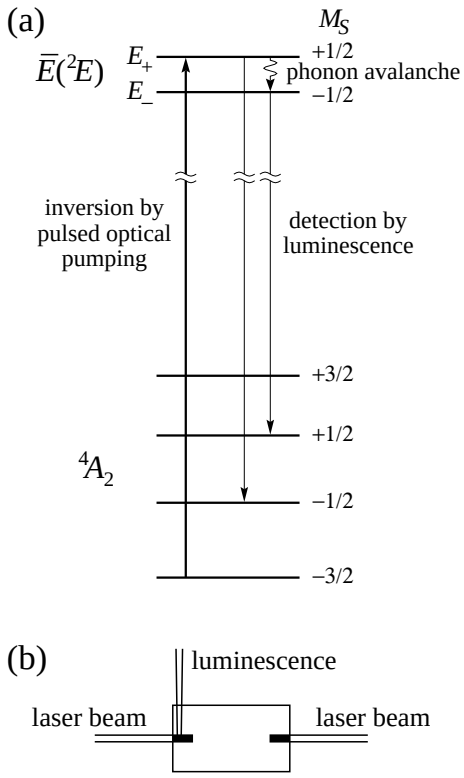

Figure 1. (a) The Zeeman-split $\overline{E}(^2E)$ and $^4A_2$ multiplets of Cr^{3+} in ruby. Pulsed optical pumping leaves the $\overline{E}(^2E)$ doublet fully population inverted. The ensuing avalanche is detected via the R_1 luminescence. (b) The two-zone experiment, with the generation zone at the right and the detection zone at the left.

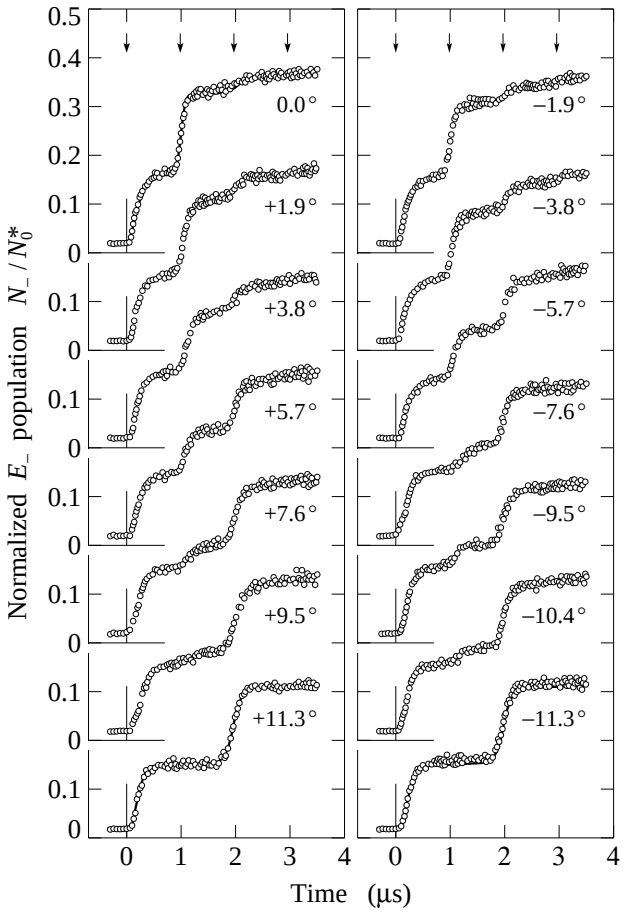

Figure 2. N_-/N_0^* in the detection zone versus the time. The traces are derived from the luminescent intensities for various lateral displacements of the generation zone. The labels denote the angle of the path connecting the zones in degrees.

mounted in a split-coil superconducting magnet, separating the $\overline{E}(^2E)$ states E_+ and E_- by $\omega/2\pi c = 1.68$ cm^{-1}, or $\nu = \omega/2\pi = 50.4$ GHz, in a field $B = 3.48$ T oriented at 65° from the c axis. The optical pumping into E_+, to a population N_0^* per unit volume, was achieved with a dye laser delivering light pulses of 8-ns duration at 50 Hz. The laser beams, whose central portions were focused to waists 200 μm in diameter, were incident along the a axis. They were polarized for maximum optical absorption, to create excited zones as short as possible ($1/e$ depth $\beta =$ 1.5 mm). The R_1 luminescence was resolved with a 0.85-m double monochromator followed by standard photon-counting techniques. The intensities of the $E_- \rightarrow {}^4A_2$, $M_S = +\frac{1}{2}$ and $E_+ \rightarrow {}^4A_2$, $M_S = -\frac{1}{2}$ transitions reflect, because of Kramers symmetry, the populations N_+ and the initially zero N_- in direct comparison. For further details on the setup reference is made to [2].

Figure 2 presents experimental traces of N_-/N_0^* in the detection zone versus the time for a series of lateral displacements of the generation zone, converted to angles using the length $L = 6.60$ mm of the crystal. These traces feature steps at intervals $L/v = 0.99$ μs, i.e., the time needed by T_1 phonons to traverse the crystal with velocity $v = 6.7$ km/s. The initial rise marks the primary avalanche, the step at L/v arrival at the opposite zone, the step at $2L/v$ return to the generation zone, and so on. The step at L/v obviously is of primary interest here.

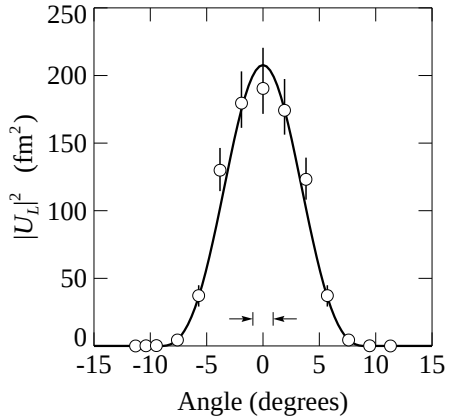

Figure 3. The squared amplitude $|U_L|^2$ of the left-propagating acoustic wave versus the angle of its trajectory. The detection zone spans an angle of 1.8°, as indicated by the arrows.

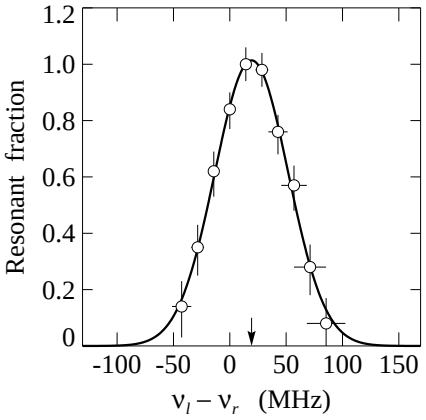

Figure 4. Fraction of N_0^* in the detection zone that is resonant with the acoustic beam leaving the generation zone versus the frequency shift. The arrow indicates the shift due to inhomogeneity of the main magnet.

The successive steps in N_-/N_0^* reflect the number of phonons released by stimulated emission as a result of incoming phonons. To extract the incoming intensity, therefore, we set up an analysis based on Bloch equations for the amplitude $U(x,t)$ of an acoustic wave traveling in, say, the x direction while coupled, with coupling constant γ, to the transverse components $S^x(x,t)$ of the Cr^{3+} spins. We decompose $U(x,t)$ into right- and left-going waves with amplitudes U_R and U_L. Similarly, we introduce right- and left-going components S_R and S_L of the transverse spin density $2N^*S^x(x,t)$. The latter expresses, through the $\overline{E}(^2E)$ population density $N^* = N_+ + N_-$, that only a fraction of the Al sites are occupied by excited Cr^{3+} ions. While $U(x,t)$ and $S^x(x,t)$ are coupled directly, they also affect, in higher order, the longitudinal spin density $2N^*S^z(x,t)$, which equals the $\overline{E}(^2E)$ population difference $n = N_+ - N_-$. The Bloch equations governing U_R, U_L, S_R, S_L, and n, which all vary slowly in time and space, take on the form [1]

$$\begin{aligned}
\partial U_R/\partial t + v(\partial U_R/\partial x) &= -(a^4\gamma\hbar/2Mv)S_R, & \partial S_R/\partial t &= -a\gamma k U_R n - S_R/T_2,\\
\partial U_L/\partial t - v(\partial U_L/\partial x) &= +(a^4\gamma\hbar/2Mv)S_L, & \partial S_L/\partial t &= +a\gamma k U_L n - S_L/T_2, \qquad (1)\\
\partial n/\partial t &= 2a\gamma k(U_R^*S_R + U_R S_R^* - U_L^*S_L - U_L S_L^*) - [(1+2p_0)n + N^*]/T_1.
\end{aligned}$$

Here, $k = \omega/v$ is the acoustic wave vector, $a \approx 0.5$ nm is the lattice constant, and $M = 3.39 \times 10^{-25}$ kg is the mass of the unit cell containing two Al_2O_3. Equations (1) include, in the customary heuristic way, thermal relaxation and spin dephasing within $\overline{E}(^2E)$. Under the present conditions, $T_1 = 0.67$ ms, $p_0 = 0.22$, and $T_2 \approx 7$ ns [1]. A reasonable estimate for γ may be derived from T_1 and the system parameters [1, 3]. The model is completed by accounting for phonon loss at the crystal boundaries by reducing $U(x,t)$ upon reflection by a reflectance $R < 1$. The Bloch equations further require a small, but finite, start-up wave amplitude U_0.

The analysis proceeds by numerical simulation of equations (1) with the appropriate position-dependent initial $\overline{E}(^2E)$ populations N_0^* in each zone. The results are subsequently fit to the measured traces in figure 2, with adjustment of N_0^*, R, and, although of no further concern, U_0. In figure 3, the resulting recalculated $|U_L|^2$ is plotted, as data points, versus the direction of travel. The measured profile has a width of about 8°. Removing the finite resolution of the detection zone, which viewed from the generation zone spans an angle of 1.8°, leaves a directionality of 3° to either side.

For comparison with theory, we calculate the divergence of the acoustic beam from the geometry of the generation zone. As initial population, we adopt the local E_+ population $N_0^*(x,y,z) = N_0^* \exp[(L-x)/\beta]$ if $y^2+z^2 \leq d^2$, and $N_0^*(x,y,z) = 0$ elsewhere. At the start of an avalanche, phonons are spontaneously emitted by Cr^{3+} residing in E_+. These phonons subsequently release further phonons by iterative stimulated emission, until phonon occupations of order 10^3 are reached. Stimulated emission, however, compels the added phonons to travel along the direction first chosen, to form a "ray" of coherent phonons. According to equations (1), these rays grow exponentially in intensity with the distance traveled times the local $N_{0,r}^*(x,y,z)$. Rays thus contribute significantly only if they traverse the zone over most of its length.

In the numerical calculations of this model, we let some 10^6 rays depart in all directions from, evenly distributed, the far end of the generation zone. These rays are subsequently amplified according to equations (1), and their contributions to $|U_L|^2$ are collected in a square matrix of finite bins at the left boundary of the crystal. This matrix is finally read out into the detector scanning across it, to find $|U_L|^2$ integrated over the detector area as a function of the angle connecting the generation and detection zones. The result is entered into figure 3 as the full curve. Fair agreement is obtained for realistic values of the parameters specifying the geometry of the generation zone as well as the acceptance area of the detection zone, viz., $\beta = 1.5$ mm and $d = 200$ μm. This leads to the conclusion that the initial divergence of the acoustic wave is governed by the geometry of the generation zone.

In a quite similar experiment, we measure the frequency distribution of the traveling acoustic wave. Instead of changing the mutual position, we apply a gradient magnetic field shifting the center frequencies between the zones. The gradient field is supplied by a split-coil, oppositely wired, superconducting minimagnet located in the sample area, whose currents are converted to differences $\nu_l - \nu_r$ in the center frequencies. The data points in figure 4 represent the experimental frequency profile. More precisely, we display, as a function of $\nu_l - \nu_r$, the normalized fraction of N_0^* in the generation zone that is resonant with $\overline{E}(^2E)$ in the detection zone. These points are derived from time traces of N_- in the detection zone similar to those in figure 2. Again, an analysis by simulating and fitting the Bloch equations (1) was necessary.

A Gaussian line shape with a full width of 77 ± 15 MHz at half maximum (full curve in figure 4) fits the data points, the offset of 19 ± 5 MHz being due to residual inhomogeneity of the static magnetic field. Both the avalanche and the luminescent detector have frequency distributions related to the $\overline{E}(^2E)$ line shape. If these are taken equal, we find for the frequency distribution of the acoustic wave a Gaussian with a full width of approximately 54 MHz at half maximum, three orders of magnitude smaller than the phonon frequency. This result compares with the $\overline{E}(^2E)$ line width from optically detected EPR [4, 5]. Sources contributing to inhomogeneous broadening of the $\overline{E}(^2E)$ transition are random magnetic fields from the nearby Al nuclear moments as well as crystalline imperfections causing wandering of the c axis, both favoring a Gaussian profile. The homogeneous component of the line width amounts to $(1+2p)/\pi T_1$, which even at the phonon occupations reached ($p \sim 10^3$) does not exceed 1 MHz. The conclusion is therefore justified that, within errors, the phonon avalanche and the associated acoustic wave are inhomogeneously broadened in keeping with the phonon transition.

References

[1] Tilstra L G, Arts A F M and de Wijn H W 2003 *Phys. Rev. B* **68** 144302
[2] Tilstra L G, Arts A F M and de Wijn H W 2007 *Phys. Rev. B* **76** 024302
[3] Leonardi C, MacGillivray J C, Liberman S and Feld M S 1973 *Phys. Rev. B* **11** 3298
[4] Geschwind S, Devlin G E, Cohen R L and Chinn S R 1965 *Phys. Rev.* **137** A1087
[5] Muramoto T 1973 *J. Phys. Soc. Japan* **35** 921